Journal of Materials Chemistry A

Accepted Manuscript

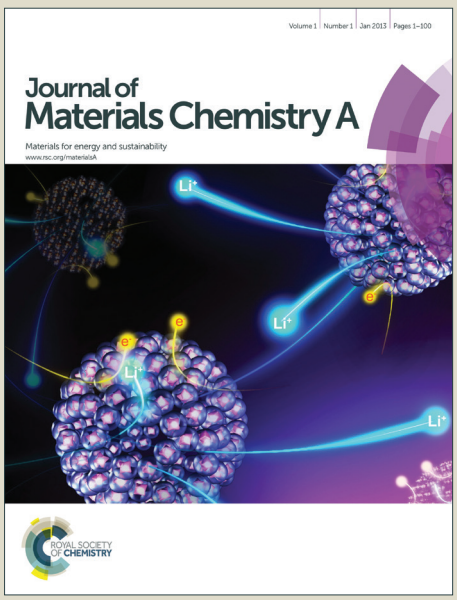

ROYAL SOCIETY OF CHEMISTRY

www.rsc.org/materialsA

Cite this: DOI: 10.1039/c0xx00000x

www.rsc.org/xxxxxx

ARTICLE TYPE

Boron-dibenzopyrromethene-based organic dyes for application in dye-sensitized solar cells

Yuji Kubo,*[a] Daichi Eguchi,[a] Asaki Matsumoto,[a] Ryuhei Nishiyabu,[a] Hidenori Yakushiji,[b] Koichiro Shigaki[b] and Masayoshi Kaneko[b]

Received (in XXX, XXX) Xth XXXXXXXXX 20XX, Accepted Xth XXXXXXXXX 20XX
DOI: 10.1039/b000000x

Novel boron-dibenzopyrromethene dyes with thienyl-cyanoacrylic acid units were synthesized and characterized for application in dye-sensitized solar cells (DSSCs); the dyes feature intense absorption bands in the longer wavelength region with λ_{max} values of 647 nm ($\varepsilon = 1.57 \times 10^5$ M^{-1} cm^{-1}) for **1**, which has two anchoring units, 660 nm ($\varepsilon = 1.09 \times 10^5$ M^{-1} cm^{-1}) for regioisomer **2**, and 644 nm ($\varepsilon = 1.39 \times 10^5$ M^{-1} cm^{-1}) for **3**, which has a single anchoring unit. Density functional theory (DFT) analysis revealed that these absorption properties are mainly characterized by intramolecular charge transfer from the dibenzopyrromethene core to the thienyl-cyanoacrylic acid unit that depend on both the number of anchoring groups and position of the thienyl-cyanoacrylic acid unit on the isoindole ring. The relationship between the chemical structures and cell properties of these dyes was investigated. Although the short circuit photocurrent density (J_{SC}) value of a **1**-loaded cell is larger than that of a **3**-loaded cell, which reflects the results of the incident photon-to-charge carrier efficiency (IPCE) spectra, the **1**-loaded cell has a lower open circuit voltage (V_{OC}) and fill factor (FF). Accordingly, overall power-to-current conversion efficiencies of 5.24 and 5.48% were obtained for a **1**-loaded cell and **3**-loaded cell, respectively, under 100 mW cm^{-2} AM1.5G simulated light. On the other hand, the cell containing butterfly-shaped regioisomer **2**, which showed improved intramolecular charge transfer, has an overall power-to-current conversion efficiency of 6.06%; this value is the highest published for BODIPY dyes even though the sensitizer does not contain any strong donor units, such as arylamines.

Introduction

Currently, in response to the substantial demand for renewable natural energy sources, devices based on dye-sensitized solar cells (DSSCs) are being intensively investigated as low-cost alternatives to traditional silicon-based photovoltaic devices.[1] Dye molecules play a significant role in the performance of DSSCs, in which sensitization of the dye via the application of solar energy onto the mesoporous photoanode excites electrons to the electrode. These electrons transfer to the counter electrode and are then shuttled back to the oxidized dye through an I^-/I_3^- redox couple. Therefore, sophisticated molecular design of dyes with efficient light-harvesting capabilities and good durability is required for the fabrication of practical cell devices.[2] 4,4-Difluoro-4-bora-3a,4a-diaza-*s*-indacene (BODIPY) dyes composed of boron-dipyrrin complexes have emerged as promising dye candidates[3] because of their outstanding properties, which include high molecular extinction coefficients of absorption, high fluorescence quantum yield, and excellent photostability. Thus, they have been applied in chemosensors,[4] biological labels,[5] organic light-emitting diodes,[6] photodynamic therapy,[7] light-harvesting arrays,[8] and solar-cell devices.[9] However, despite the extensive research into the development of DSSC devices based on BODIPY sensitizers,[10] the power-to-current conversion efficiency (PCE) value is currently limited at less than 2.46%.[10f] The development of a new design for a BODIPY-based π-system remains a major challenge despite their excellent optical properties and facile structural modification via a variety of synthetic methods.

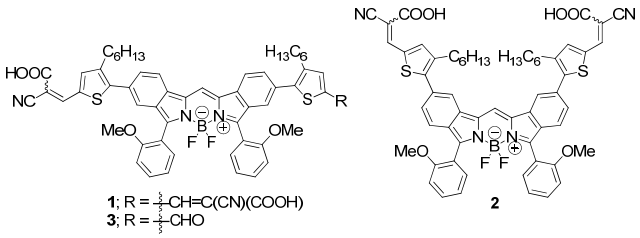

Fig. 1 Chemical structures of dyes **1**, **2** and **3**.

Our ongoing effort to prepare dye materials that absorb longer wavelengths of radiation led us to modify the structure of BODIPY by extending the π-conjugation to provide new types of boron-dibenzopyrromethene dyes.[11] The synthetic route that we employ enables the development of hexylthiophene-conjugated boron-dibenzopyrromethenes with near-infrared light absorption bands that serve as photosensitizers in bulk heterojunction solar cells.[12] We realized that the synthetic improvement of such a

chromophoric system could enable it to act as a potent sensitizer in DSSC devices. Accordingly, cyanoacrylic acid, which acts as both an anchor to the TiO_2-based electrode and electron acceptor, was incorporated into the core skeleton through the π-bridge of hexylthiophene. The hexyl group at the γ-position of the thiophene ring weakens the intramolecular interactions of the dyes. In this study, two regioisomers with two anchoring units, i.e., **1** and **2**, were designed and synthesized by introducing an anchoring group at the 5 or 6 position of the isoindole ring of the dye and characterized (Fig. 1). Further, during synthesis of **1**, dye **3**, which has a single anchoring unit, was unexpectedly isolated (*vide infra*, Scheme 1). The characterization of **3** as a sensitizer is important to understanding the DSSC performance of a **1**-loaded cell. As described below in detail, we discovered that both the number of anchoring groups and position of the anchoring group impact the cell properties. Accordingly, the DSSC device containing butterfly-shaped **2** has improved photovoltaic performance.

Experimental section

General

NMR spectra were taken by a JEOL JNM-ECS 300 (^{1}H: 300 MHz) or a Bruker Avance 500 (^{1}H: 500 MHz, ^{13}C: 125 MHz, ^{19}F: 470 MHz) spectrometers. In ^{1}H and ^{13}C NMR measurements, chemical shifts (δ) are reported downfield from the initial standard Me_4Si. While in ^{19}F NMR measurement, hexafluorobenzene was used as an internal standard (−164.9 ppm). In addition, fast atom bombardment (FAB) mass spectra were obtained on a JEOL JMS-700 spectrometer where *m*-nitrobenzyl alcohol was used as a matrix. The absorption spectra were measured using a Shimadzu UV-3600 spectrophotometer. Elemental analyses were performed on a Exeter Analytical, Inc. CE-440F Elemental Analyzer. Infrared spectra were recorded on JASCO FT/IR-4100.

Materials

Reagents used for the synthesis were commercially available and used as supplied. Dry-THF, EtOH, and toluene were prepared according to standard procedure. Difluoro[5-bromo-1-[[5-bromo-3-(2-methoxyphenyl)-2*H*-isoindole-l-yl]methylene]-3-(2-methoxyphenyl)-1*H*-isoindolate-N^1,N^2]boron (**4**) was prepared from 4-bromo-2-hydroxyacetophenone through 4 steps.[12] 2-(5-(5,5-Dimethyl-1,3-dioxan-2-yl)-3-hexylthiophen-2-yl)-4,4,5,5-tetramethyl-1,3,2-dioxaborolane (**5**) was also prepared from 2-bromo-3-hexyl-5-formylthiophene[13] through protection of aldehyde using neopentyl glycol, followed by borylation with 2-isopropoxy-4,4,5,5-tetramethyl-1,3,2-dioxaborolane in the presence of *n*-BuLi; ^{1}H NMR of **5** (300 MHz, $CDCl_3$) δ (ppm) 0.78 (s, 3H), 0.87 (t, 3H, *J* = 6.40 Hz), 1.25 (s, 3H), 1.25–1.36 (m, 18H), 1.50–1.59 (m, 2H), 2.81 (t, 2H, *J* = 7.62 Hz), 3.61 (d, 2H, *J* = 10.89 Hz), 3.73 (d, 2H, *J* = 11.01 Hz), 5.59 (s, 1H), 7.04 (s, 1H), FAB MS : *m*/*z* 407 $[M-1]^+$, 408$[M]^+$. Details of synthetic procedures for the intermediate compounds **6–14** are described in Electronic Supporting Information.

Synthesis

Difluoro[5-(3-hexyl-5-(2-carboxy-2-cyanovinyl)thiophen-2-yl)-1-[[5-(3-hexyl-5-(2-carboxy-2-cyanovinyl)thiophen-2-yl)-3-(2-methoxyphenyl)-2*H*-isoindole-1-yl]methylene]-3-(2-methoxyphenyl)-1*H*-isoindolate-N^1,N^2]boron (1) and Difluoro[5-(3-hexyl-5-(2-carboxy-2-cyanovinyl)thiophen-2-yl)-1-[[5-(3-hexyl-5-formylthiophen-2-yl)-3-(2-methoxyphenyl)-2*H*-isoindole-l-yl]methylene]-3-(2-methoxyphenyl)-1*H*-isoindolate-N^1,N^2]boron (3)

To a solution of **7** (501 mg, 0.561 mmol) and piperidine (0.28 mL, 2.83 mmol) in THF (14 mL) was added a solution of 2-cyanoacetic acid (242 mg, 2.84 mmol) and piperidine (0.28 mL, 2.83 mmol) in THF (14 mL). The resulting solution was refluxed for 5 h and then poured into H_2O (100 mL). After extraction with CH_2Cl_2 (100 mL), the organic layer [A] was washed with brine (100 mL) and water (100 mL). Such a treatment led to precipitation of green solid being filtered off. After dissolving the material in CH_2Cl_2 (400 mL), the resulting solution was washed with 1% HCl aq. (100 mL) and was evaporated. In this way, 246 mg of **1** was obtained in 43% yield. On the other hand, the filtrate of the organic layer [A] was dried with Na_2SO_4 and was evaporated. The residue was chromatographed on silica gel (Wacogel C-300) using a gradient of EtOH (0–10% v/v) in CH_2Cl_2 as an eluent to give **3** in 40% yield. For **1**; ^{1}H NMR (500 MHz, DMSO-d_6) δ (ppm) 0.79 (t, 6H, *J* = 6.77 Hz), 1.14–1.20 (m, 12H), 1.48–1.59 (m, 4H), 2.62–2.66 (m, 4H), 3.69 (s, 3H), 3.76 (s, 3H), 7.03 (t, 1H, *J* = 7.53 Hz), 7.10 (t, 1H, *J* = 7.47 Hz), 7.20 (d, 1H, *J* = 8.30 Hz), 7.24 (d, 1H, *J* = 8.45 Hz), 7.37 (s, 1H), 7.39 (s, 1H), 7.45 (d, 1H, *J* = 7.50 Hz), 7.51 (t, 3H, *J* = 8.18 Hz), 7.71 (d, 2H, *J* = 8.45 Hz), 7.94 (s, 2H), 8.30 (d, 1H, *J* = 8.30), 8.31 (d, 1H, *J* = 8.20 Hz), 8.43 (s, 2H), 8.84 and 8.85 (s, 1H), 13.75 (broad signal, 2H); ^{13}C NMR (125 MHz, DMSO-d_6) δ (ppm): 163.5, 157.3, 157.2, 150.0, 149.8, 148.8, 147.0, 146.4, 142.4, 140.2, 133.5, 132.9, 132.8, 132.0, 131.7, 131.6, 131.3, 130.3, 130.2, 129.9, 129.4, 127.2, 127.1, 123.4, 123.3, 120.7, 120.2, 120.0, 118.7, 118.5, 118.1, 118.0, 117.7, 116.4, 111.5, 98.6, 55.6, 30.9, 30.0, 28.2, 27.8, 21.9, 13.8; ^{19}F NMR (470 MHz, $CDCl_3$: DMSO-d_6 (3:7 v/v)) δ (ppm) −149.1 (J_{BF} = 29.0 Hz, $^2J_{FF}$ = 94.6 Hz), −134.8 (J_{BF} = 30.3 Hz), −121.1 (J_{BF} = 32.7 Hz, $^2J_{FF}$ = 95.7 Hz); FAB MS: *m*/*z* 1026 $[M]^+$; Elemental analysis: Calcd for $C_{59}H_{53}BF_2N_4O_6S_2 \cdot H_2O$: C, 67.81; H, 5.30; N, 5.36, found: C, 67.70; H, 5.15; N, 5.34. For **3**; ^{1}H NMR (500 MHz, DMSO-d_6) δ (ppm) 0.79 (t, 6H, *J* = 6.90Hz), 1.14–1.19 (m, 12H), 1.48–1.59 (m, 4H), 2.61–2.66 (m, 4H), 3.69 (s, 3H), 3.75 and 3.76 (s, 3H), 7.03 (t, 1H, *J* = 7.45 Hz), 7.10 (t, 1H, *J* = 7.53 Hz), 7.19 (d, 0.5H, *J* = 8.70 Hz), 7.20 (d, 0.5H, *J* = 8.25 Hz), 7.23 (d, 0.5H, *J* = 8.70 Hz), 7.23 (d, 0.5H, *J* = 8.40 Hz), 7.35–7.38 (m, 2H), 7.44 (t, 1H, *J* = 6.05 Hz), 7.49–7.52 (m, 3H), 7.68–7.72 (m, 2H), 7.90 (s, 1H), 7.97 and 7.98 (s, 1H), 8.29 (d, 1H, *J* = 8.35Hz), 8.30 (d, 1H, *J* = 8.45 Hz), 8.38 (s, 1H), 8.83 and 8.84 (s, 1H), 9.87 (s, 1H), 13.77 (broad signal, 1H); ^{13}C NMR (125 MHz, DMSO-d_6) δ (ppm) : 183.9, 163.4, 157.3, 157.2, 150.0, 149.7, 146.7, 140.8, 140.5, 140.2, 140.0, 133.8, 132.9, 132.8, 132.1, 132.0, 131.6, 131.3, 131.2, 130.3, 130.1, 130.0, 129.7, 129.5, 127.2, 127.1, 123.3, 123.2, 120.8, 120.7, 120.2, 120.0, 118.8, 118.5, 118.0, 117.9, 111.5, 55.6, 30.9, 30.0, 28.3, 28.0, 27.8, 21.9, 13.9; ^{19}F NMR (470 MHz, $CDCl_3$: DMSO-d_6 (3:7 v/v)) δ (ppm) −148.0 (J_{BF} = 28.1 Hz, $^2J_{FF}$ = 95.2 Hz), −133.7 (J_{BF} = 30.9 Hz), −133.6 (J_{BF} = 30.9 Hz), −120.8 (J_{BF} = 32.5 Hz, $^2J_{FF}$ = 94.9 Hz); FAB MS: *m*/*z* 959 $[M]^+$; Elemental analysis: Calcd for $C_{56}H_{52}BF_2N_3O_5S_2 \cdot 0.5H_2O$: C, 69.41; H, 5.51; N, 4.34, found: C, 69.08; H, 5.43; N, 4.33.

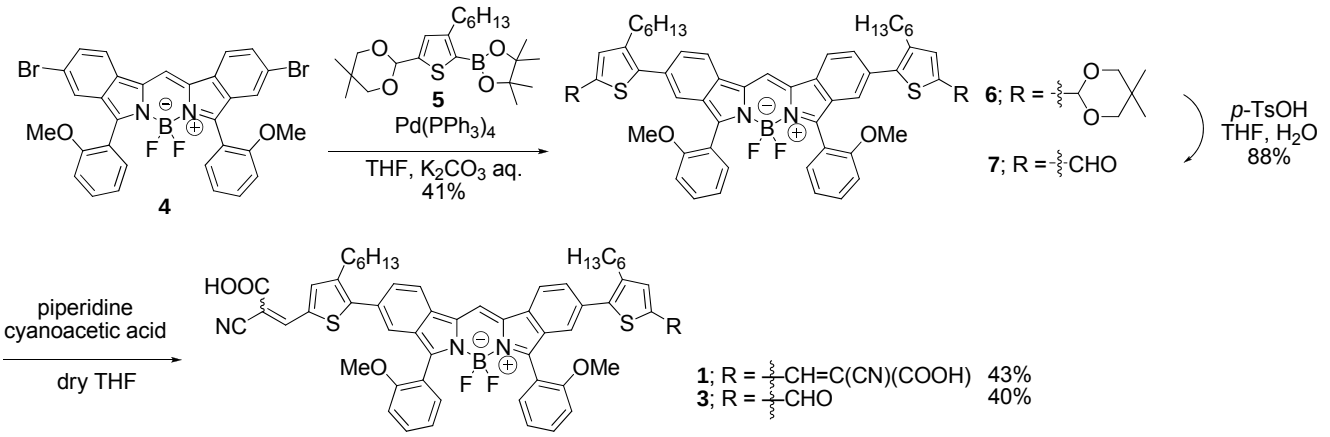

Scheme 1 Synthesis of sensitizers **1** and **3**.

Difluoro[6-(3-hexyl-5-(2-carboxy-2-cyanovinyl)thiophen-2-yl)-1-[[6-(3-hexyl-5-(2-carboxy-2-cyanovinyl)thiophen-2-yl)-3-(2-methoxyphenyl)-2*H*-isoindole-1-yl]methylene]-3-(2-methoxyphenyl)-1*H*-isoindolate-N^1,N^2]boron (2)

To a solution of compound **14** (266 mg, 0.298 mmol) and piperidine (0.2 mL, 2.03 mmol) in dry THF (7.8 mL) was added a solution of 2-cyanoacetic acid (159 mg, 1.87 mmol) and piperidine (0.2 mL, 2.03 mmol) in dry THF (7.8 mL). The mixture was refluxed for 2 days. The addition of CH_2Cl_2 (30 mL) into the resulting solution gave a precipitate, followed by extraction using CH_2Cl_2 (100 mL) and 1 N HCl aq. (100 mL). The organic layer was then dried with Na_2SO_4 and evaporated *in vacuo*. The resulting residue was reprecipitated with CH_2Cl_2 (10 mL)/hexane (100 mL) to give **2** as a conformation mixture ($\Delta G^{\neq}$ = 76.5 kJ mol^{-1}) in 65% yield. ^{1}H NMR (500 MHz, DMSO-d_6) δ (ppm) 0.76 (t, 6H, J = 6.93 Hz), 1.19–1.26 (m, 12H), 1.60 (quint, 4H, J = 7.24 Hz), 2.78 (t, 4H, J = 7.35 Hz), 3.70 (s, 3H), 3.75 (s, 3H), 7.03 (t, 1H, J = 7.75 Hz), 7.09 (t, 1H, J = 7.70 Hz), 7.20 (d, 1H, J = 8.35 Hz), 7.24 (d, 1H, J = 8.35 Hz), 7.38–7.46 (m, 5H), 7.49 (d, 1H, J = 7.25 Hz), 7.51 (t, 2H, J = 8.02 Hz), 8.03 (s, 2H), 8.32 and 8.33 (s, 2H), 8.51 (s, 2H), 8.90 and 8.91 (s, 1H), 13.77 (s, 2H); ^{13}C NMR (125 MHz, DMSO-d_6) δ (ppm) 163.4, 157.4, 157.3, 149.1, 148.8, 147.0, 146.5, 142.5, 140.7, 133.9, 133.5, 131.9, 131.5, 131.2, 129.7, 127.4, 125.8, 124.0, 120.2, 120.0, 119.9, 118.9, 118.7, 117.5, 116.2, 111.5, 98.7, 55.5, 30.7, 29.7, 28.1, 27.7, 21.9, 13.7; ^{19}F NMR (470 MHz, $CDCl_3$:DMSO-d_6 (3:7 v/v)) δ (ppm) −148.4 (J_{BF} = 28.1 Hz, $^2J_{FF}$ = 95.8 Hz), −134.4 (J_{BF} = 30.7 Hz), −121.2 (J_{BF} = 34.1 Hz, $^2J_{FF}$ = 95.8 Hz); FAB MS: *m/z* 1026 $[M]^+$; Elemental analys: Calcd for $C_{59}H_{53}BF_2N_4O_6S_2 \cdot 0.5H_2O$: C, 68.40; H, 5.25; N, 5.41, found: C, 68.24; H, 5.08; N, 5.33.

Electrochemical measurements

Cyclic voltammograms (CV) were recorded on a Princeton Applied Research VersaSTAT 3 potentiostat operated at a scan rate of 50 mV s^{-1} and room temperature under a N_2 atmosphere. The solvent was DMF/CH_2Cl_2 (1:4 v/v) containing 0.1 M tetrabutylammoniumhexafluorophosphate ($TBAPF_6$) as the supporting electrolyte. The potentials were measured against Ag/Ag^+ (0.01 M of $AgNO_3$) as a reference electrode; ferrocene/ferrocenium (Fc/Fc^+) was used as the internal standard and measured to be 0.06 V under same conditions. The onset potentials were determined from the intersection of two tangents drawn at the rising and background currents of the cyclic voltammogram.

Theoretical calculation

All geometries of the dyes at the ground state were fully optimized by means of AM1 method. The structural geometry was optimized by AM1 method. Density functional theory (DFT) calculations at the CAM-B3LYP/6-31G(d,p) level were performed in the Gaussian 09 package. The molecular orbitals in Fig. 4 were visualized using Gauss view 5.0.8 program.

Fabrication of dye-sensitized solar cell device

The nanoporous TiO_2 was deposited on a fluorine-doped-tin-oxide (FTO) substrate and sintered for 1 h at 500 °C. The 10 μm-thick TiO_2 electrode was immersed into acetone solution of dye sensitizers (1.6×10^{-4} M) and deoxycholic acid (10 mM) for 12 h at room temperature. The resultant dye-absorbed TiO_2 electrode was applied for DSSC device with a platinized counter electrode and a liquid electrolyte comprising I_2 (0.1 M), LiI (0.1 M), and dimethylpropylimidazolium iodide (0.6 M) in methoxypropionitrile. The photocurrent-voltage characters were measured on a sourcemeter (6243, ADC Co. LTD) under 100 mW cm^{-2} AM1.5G simulated solar light (WXS-155S-10, WACOM electric Co. LTD). The incident photon–to–charge carrier efficiencies (IPCEs) measured on IPCE Measurement System (SM-250, Bunkoukeiki Co., Ltd.).

Results and Discussions

The synthetic path that we employed in this study enables the introduction of a bromo substituent at the 5 or 6 position of the isoindole ring via the choice of starting material; thus, two regioisomers of the target sensitizers could be generated. Accordingly, we investigated the regio-dependency of both the optical properties and performance of DSSCs based on these dyes. Indeed, the dipole moment ($\Delta\mu$) of **2** was determined to be 13.243 D from DFT calculations; this value is 3.0 times larger than that of **1** (Table 1) and results in improved DSSC performance.

The synthetic route to the target sensitizer, **1**, is shown in Scheme 1. The starting material, i.e., 5,5-dibromo- and bis(anisole)-substituted boron-dibenzopyrromethene difluoride **4**,[12] coupled with acetal-protected borylthiophene derivative **5**

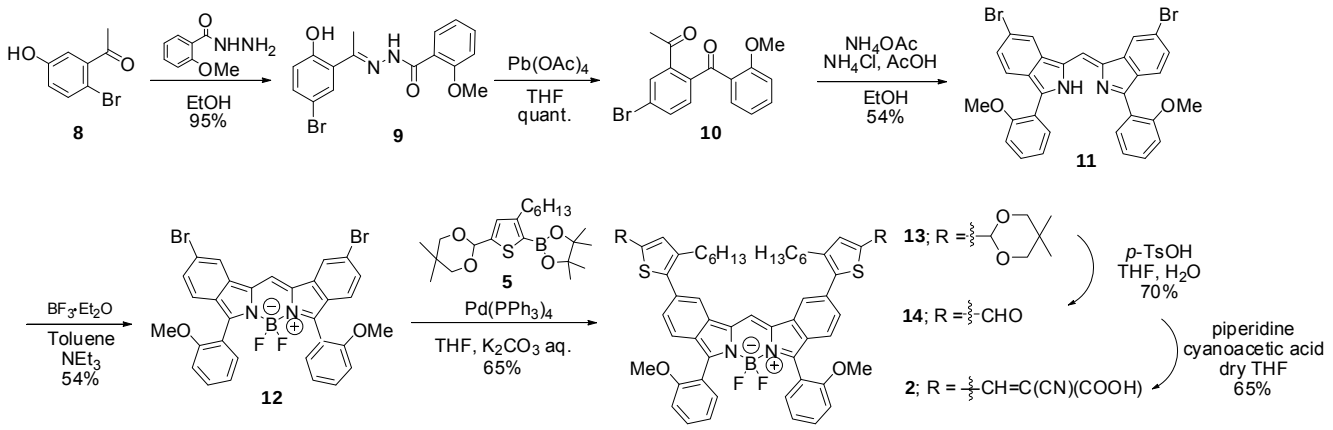

Scheme 2 Synthesis of sensitizer **2**.

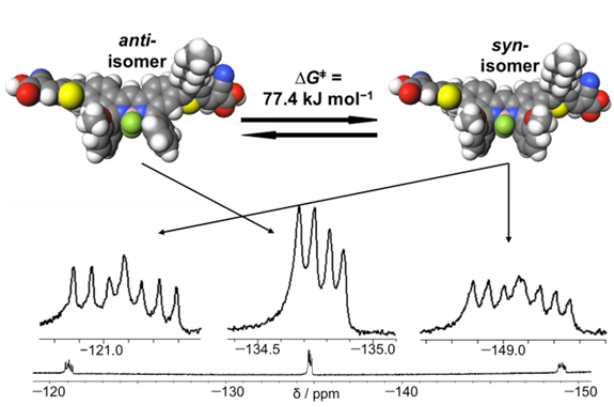

Fig. 2 Proposed conformers of **1** and their ^{19}F NMR spectra in DMSO-d_6:$CDCl_3$ (3:7 v/v) at room temperature.

followed by deprotection with *p*-TsOH to afford **7**. Finally, **7** underwent Knoevenagel condensation with five equivalents of cyanoacetic acid in the presence of piperidine. Stirring the mixture for 5 h under reflux generated target **1** and **3**, which contains an unreacted formyl group, in 43 and 40% yields, respectively. Structural assignments were performed via NMR, FAB MS, and elemental analysis. The ^{1}H NMR spectrum of **1** in DMSO-d_6 at room temperature contains two set of signals assignable to the anisole segment: Proton resonances arising from the methoxy groups were detected at 3.69 and 3.76 ppm (Fig. S1(a)). VT-NMR analysis revealed a T_c value of 94 °C, which suggests that two conformers of **1** coexist under ambient conditions. To gain further insight into the structures, we recorded a ^{19}F NMR spectrum of **1** in DMSO-d_6:$CDCl_3$ (3:7 v/v), which revealed a quintet signal at −134.8 ppm (J_{BF} = 30.3 Hz) and octet signals at −121.1 ppm (J_{BF} = 32.7 Hz, $^2J_{FF}$ = 95.7 Hz) and −149.1 ppm (J_{BF} =29.0 Hz, $^2J_{FF}$ = 94.6 Hz), as shown in Fig. 2; this indicates that *anti*- and *syn*-isomers, in which the anisole moieties are located on the opposite and same face of the dibenzopyrromethene core, respectively, are stable under ambient conditions ($\Delta G^{\neq}$ = 77.4 kJ mol^{-1}). This is intriguing because simple bis(anisole)-appended BODIPY does not have conformational isomers.[14] The isoindole ring in **1** may restrict rotation about the two $C_{anisole}$–$C_{isoindole}$ bonds. Attempts at separating these isomers using silica gel chromatography were

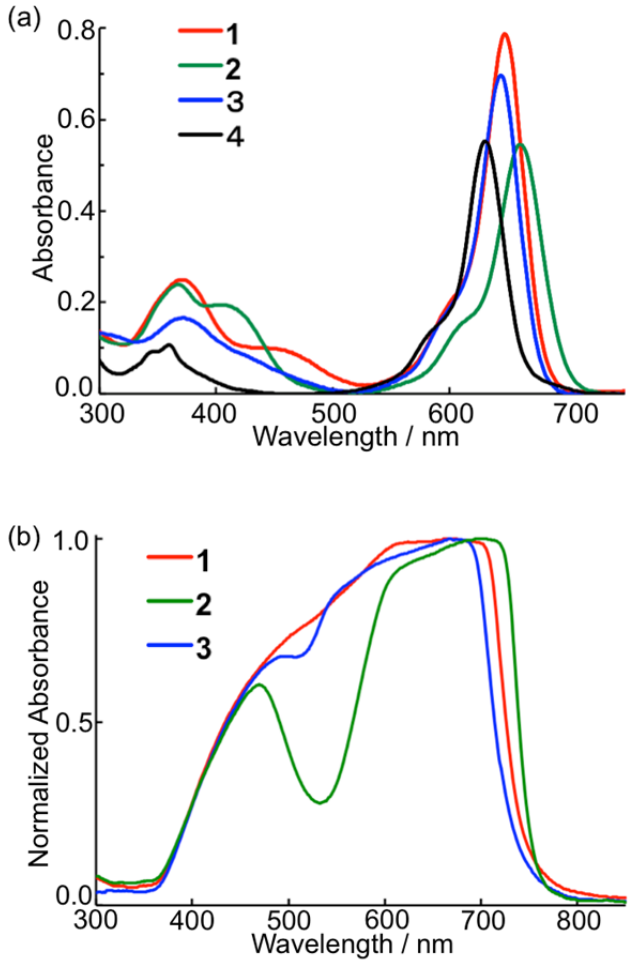

Fig. 3 (a) Absorption spectra of dyes in THF (5 μM); (b) Normalized absorption spectra of dyes on 10 μm thin TiO_2 film.

unsuccessful. The sensitizers prepared in this study comprise such a conformational mixture at room temperature. A similar phenomenon was observed for **3** ($\Delta G^{\neq}$ = 78.5 kJ mol^{-1} in Fig. S1(c)).

Scheme 2 shows the synthetic route to **2**: Initially, 6,6'-dibromo-substituted boron-dibenzopyrromethene **12**, which was prepared from 2-acetyl-4-bromophenol **8** via a four-step

Table 1 Optical properties and theoretical data for dyes **1–4**.

Dye	λ_{max} / nm (ε / 10^5 M^{-1} cm^{-1})[a]	λ_{max} (Calcd) / nm[b]	Calculated assignment	f (Calcd)[c]	$\Delta\mu$ /Debye[c]
1	647 (1.57), 457 (0.192), 371 (0.500)	529	HOMO → LUMO (46.8%)[d] HOMO → LUMO +2 (1.6%)	1.5550	4.486
2	660 (1.09), 406 (0.390), 369 (0.478)	542	HOMO → LUMO (43.7%)[d] HOMO → LUMO +1 (1.2%) HOMO → LUMO +2 (3.6%)	1.0846	13.243
3	644 (1.39), 371 (0.332)	527	HOMO → LUMO (45.3%)[d] HOMO → LUMO +1 (3.3%)	1.3939	4.046
4	631 (1.11), 360 (0.212)	523	–	0.9299	–

[a]The absorption maxima (λ_{max}) and molecular extinction coefficients (ε) were measured in THF. [b]The longest wavelength absorption bands, which was calculated using CAM-B3LYP/6-31G(d,p) level.[c]Calculated using CAM-B3LYP/6-31G(d,p) level. [d](CI cofficient)^2 × 100%[15]

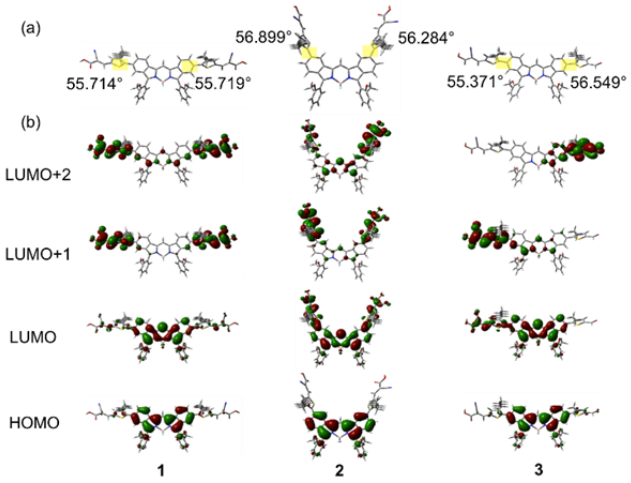

Fig. 4 (a) Molecular geometries of **1**, **2** and **3** with dihedral angles between isoindole ring and thiophene π-spacer indicated, and (b) surface plots, as estimated from DFT calculations (CAM-B3LYP/6-31G (d,p)).

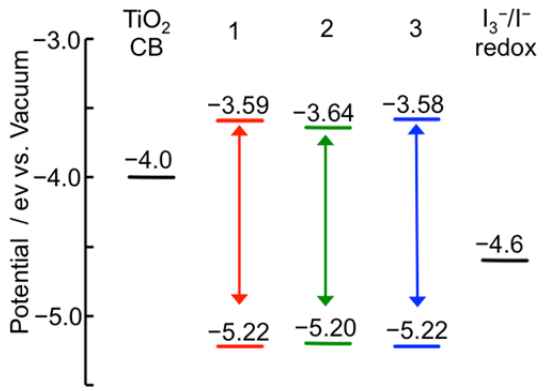

Fig. 5 HOMO and LUMO energy levels of **1**, **2** and **3**. The energy levels were calculated from the CV measurements in DMF/CH_2Cl_2 (1:4 v/v) containing 0.1 M $TBAPF_6$; HOMO [eV] = − (E_{ox} − $E_{Fc/Fc+}$ + 4.8); LUMO [eV] = − (E_{red} − $E_{Fc/Fc+}$ + 4.8).

synthesis, underwent Suzuki cross-coupling with **5**, deprotection with *p*-TsOH, and Knoevenagel condensation with cyanoacetic acid to afford butterfly-shaped regioisomer **2** as a conformational mixture of *anti*- and *syn*-mixtures ($\Delta G^{\neq}$ = 76.5 kJ mol^{-1} in Fig. S1(b)).

We were interested in how the slight differences in the structures of these dyes would affect the electronic properties of the sensitizers. Our first insight into this subject came from the UV-vis absorption spectra shown in Fig. 3a, which includes the spectrum of 5,5-dibromo derivative **4** (Scheme 1) as a reference: Dye **1** absorbs visible light with a λ_{max} of 647 nm and has a relatively large molecular extinction coefficient (ε) of 1.57 × 10^5 M^{-1} cm^{-1} as a result of the π-extended BODIPY chromophore. Comparison of the UV-vis spectra of **1** and **4** reveals that insertion of cycanoacrylic acid as an accepting group via a thiophene π-bridge causes a bathochromic shift of 16 nm and increased absorption intensity. The first absorption band of **3**, which has an unreacted formyl group, is slightly blue-shifted and has a lower absorption intensity relative to that of **1**. On the other hand, regioisomer **2** exhibits distinct absorption properties (λ_{max} = 660 nm, ε = 1.09 × 10^5 M^{-1} cm^{-1}) with a 13 nm red-shifted λ_{max} relative to that of **1**. Also, dyes **1**, **2**, and **3** have a relatively small, but still significant, absorption band at 320 to 500 nm. This spectral feature is valuable for DSSC applications because it would contribute to their light-harvesting efficiency as sensitizers (*vide infra*). For a better understanding of the absorption properties, the transition energies and oscillator strengths (*f*) were calculated based on time-dependent density functional theory (TD-DFT) at the CAM-B3LYP/6-31G(d,p) level. The trend of the calculated λ_{max} values in the first absorption band is almost consistent with that of the spectra recorded in THF despite the twist in the structure between the isoindole ring and thiophene π spacer (dihedral angle of ~56° (Fig. 4a)). The electron-density distributions of these dyes are illustrated for the following molecular orbitals: HOMO, LUMO, LUMO+1, and LUMO+2 (Fig. 4b). Although the maximum absorption band is mainly ascribed to a HOMO–LUMO transition, it is characterized as a mixture of several configurations (Table 1). The electron-density distributions of the HOMOs of the dyes are mainly localized on the dibenzopyrromethene core. Although the LUMO and higher LUMO orbitals of the dye core are populated with electron density, a significant amount of electron density extends toward the thienyl-cyanoacrylic acid units. It appears that the LUMO and higher LUMO orbitals synchronize to inject electrons into the conduction band of TiO_2. Accordingly, the excitation is dominated by intramolecular charge transfer (ICT) from the HOMO to the LUMO and higher LUMO orbitals, which is reflected in the absorption properties of the dyes in the longer wavelength region. Further, the electron density on the cyanoacrylic acid moiety in the LUMO of **2** is greater than that in the LUMO of **1**. The theoretical data indicate that the electronic properties are dependent on the position of the thienyl-cyanoacrylic acid moiety on the isoindole ring, which may be associated with the effectiveness of ICT. Indeed, **2** has a higher

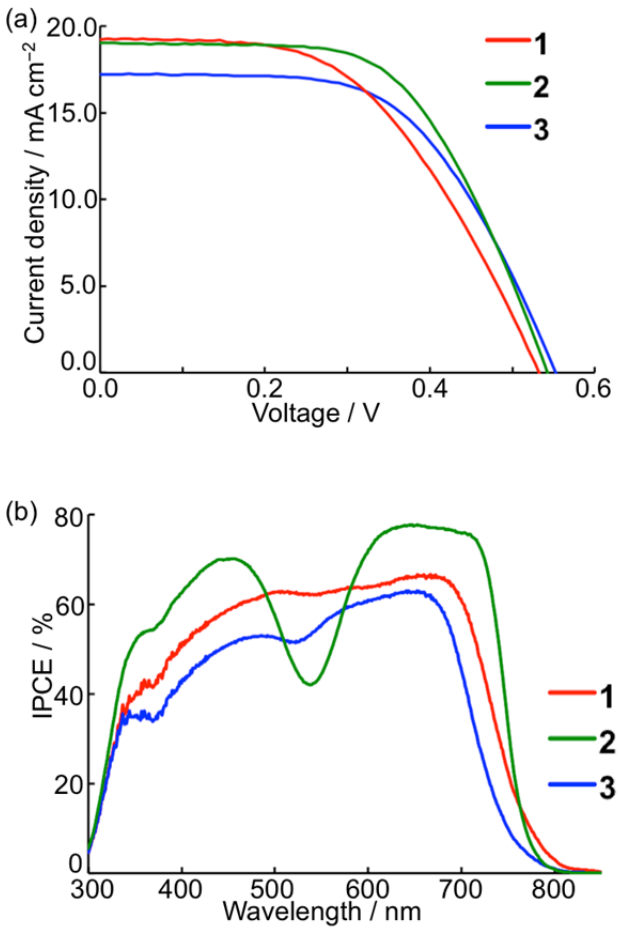

Fig. 6 (a) Photocurrent density–voltage (*J*–*V*) curves and (b) IPCE action spectra of dye-loaded cells.

dipole moment (*vide supra*).

The electrochemical properties of the sensitizers were measured at room temperature using cyclic voltammetry (CV) in a DMF/CH_2Cl_2 (1:4 v/v) mixture containing 0.1 M tetrabutylammonium hexafluorophosphate ($TBAPF_6$) as the supporting electrolyte (Fig. S2). The measurements were calibrated against ferrocene (−4.8 eV) as the standard.[16] The formal potential of Fc/Fc^+ was measured to be 0.06 V versus Ag/Ag^+. Although the voltammogram of **1** is almost identical to that of **3**, the electrochemical properties of **1** differ from those of regioisomer **2** (Fig. S2). The anodic scan revealed onset oxidation potentials for **1** and **2** of 0.49 and 0.47 V, respectively, which correspond to ionization potentials (HOMO levels) of −5.22 eV for **1** and −5.20 eV for **2** (Fig. 5); these values are more positive than the redox potential (−4.6 eV) of I^-/I_3^- for dye regeneration. Similarly, the onset reduction potential of these dyes enabled estimation of the electron affinities (LUMO level) for **1** and **2** (−3.59 and −3.64 eV, respectively). The LUMO is more sensitive than the HOMO to the position of the thienyl-cycanoacrylic acid moiety, which implies that the anchoring unit at the 6 position in **2** has a greater impact on the electron-withdrawing ability of the chromophore than that at the 5 position in **1**, resulting in improved ICT. The LUMO levels of these dyes are negative relative to the conduction band of TiO_2 (−4.0 eV),[17] ensuring efficient electron injection from the excited state of the dyes into

Table 2 Photovoltaic parameters of DSSC based on **1–3** under the simulated AM1.5G sunlight (100 mW cm^{-2}).[a]

Dye	J_{sc} / mA cm^{-2}	V_{oc} / V	FF	η / %
1	19.24	0.53	0.514	5.24
2	19.02	0.54	0.590	6.06
3	17.21	0.55	0.579	5.48

[a]Electrolyte: I_2 (0.1 M), LiI (0.1 M), and dimethylpropylimidazolium iodide (0.6 M) in methoxypropionitrile.

the TiO_2 electrode. Accordingly, this energetically favorable process enables application of these dyes as potential sensitizers in DSSCs (Fig. 5). The absorption spectra of the dyes were also measured on 10 μm thick TiO_2 films (Fig. 3b). Compared to the absorption bands observed in solution, the spectra on TiO_2 were broader with significant red-shifting of the absorptions; this is presumably caused by *J*-aggregation of the dyes anchored on the TiO_2 films.[18] It is interesting to note that the absorption profiles on TiO_2 film are not affected by the number of thienyl-cyanoacrylic acid units. We investigated the interactions between the carboxylic acid groups and TiO_2 using infrared (IR) absorption spectroscopy equipped with an attenuated total reflection (ATR) apparatus. The characteristic signal at 1680 cm^{-1} is attributed to the free carboxylic groups of **1**; in contrast, the IR absorption spectrum of the **1**-loaded TiO_2 film features a new absorption band at 1590 cm^{-1} and an almost negligible peak at 1680 cm^{-1} (Fig. S3). This result suggests that both cyanoacrylic acid moieties in **1** participate in binding to TiO_2. On the other hand, the absorption profile of regioisomer **2** differs from those of **1** and **3**, which suggests that the position of the anchoring unit on the isoindole ring affects the orientation of the dyes on the TiO_2 surface.

DSSCs based on these dyes were fabricated using a liquid electrolyte comprising I_2 (0.1 M), LiI (0.1 M), and dimethylpropylimidazolium iodide (0.6 M) in methoxypropionitrile. The short circuit photocurrent density (J_{SC}), open-circuit voltage (V_{OC}), and fill factor (FF) values under 100 mW cm^{-2} AM1.5G irradiation were determined from the photocurrent density–voltage (*J*–*V*) curves of the cells in the presence of deoxycholic acid as a co-adsorbent (Fig. 6a). The DSSC based on **1**, which has two anchoring units, features J_{sc}, V_{oc}, and FF values of 19.24 mA cm^{-2}, 0.53 V, and 0.514, respectively. The power-to-current conversion efficiency (η) was calculated to be 5.24% using the following equation: $\eta = J_{SC} \times V_{OC} \times FF$.[19] It is worth emphasizing that the J_{SC} of the cell is greater than 19.0 mA cm^{-2}. In contrast, the cell based on **3**, which has a single anchoring unit, has a lower J_{SC} of 17.21 mA cm^{-2}. To verify the results, the incident photon-to-charge carrier efficiencies (IPCEs), which usually depend on light-absorption photoinduced electron injection into TiO_2 and charge recombination, were measured. Fig. 6b shows the IPCE intensity plotted as a function of the incident wavelength for the DSSCs. All cells tested can convert the light to photocurrents in the wide wavelength region up to about 800 nm. The cell containing **1** exhibited a considerably broader and higher IPCE of 60% in the range of 500–700 nm, while the **3**-based cell displays an IPCE spectrum with a similar spectral pattern but slightly blue-shifted and with a lower maximum. The broader IPCE curves are consistent with the trend of the absorption spectra on TiO_2 films, and occur because **1** can

bind to the surface of TiO_2 in several ways. In contrast, the V_{oc} of the **3**-based cell (0.55 V) was slightly higher than that of the **1**-based cell, suggesting that introduction of two anchoring units does not improve the V_{OC}. The η of the **3**-based cell was estimated to be 5.48% (Table 2). In contrast, the **2**-loaded cell has a J_{sc} of 19.02 mA cm^{-2}, V_{oc} of 0.54 V, FF of 0.590, and η of 6.06%. The IPCE value of the **2**-loaded cell is higher than that of the cell loaded with **1** in the ranges of 300–490 and 580–760 nm. These results demonstrate that cell performance is affected by the position of the thienyl-cyanoacrylic acid unit on the isoindole ring. Considering the absorption profiles on TiO_2 (Fig. 3b), the ICPE spectrum likely reflects the orientation of the dye on the surface. Thus, it is evident that the use of sensitizer **2**, which has a larger dipole moment than **1**, results in improved V_{OC} and FF values under the investigated conditions.

Conclusions

In conclusion, we synthesized and characterized a series of boron-dibenzopyrromethene dyes that contain thienyl-cyanoacrylic acid units, i.e., **1**–**3**, for potential use as sensitizers in DSSC devices. The good light-harvesting abilities of the dyes led to high J_{SC} values for these dyes-loaded cells. As a result, the cell with containing butterfly-shaped **2** provided a good power-to-current conversion efficiency of 6.06%, which, to the best of our knowledge, is the highest value for BODIPY-based DSSCs reported to date. It is noteworthy that these sensitizers do not contain strong donor units, such as arylamines; this is beneficial for the design of organic sensitizers because various arylamines, such as triarylamine and carbazole, have been widely employed as strong donors in D–π–A systems in DSSCs.[20] We believe that the use of boron-dibenzopyrromethene as a core skeleton in metal-free organic sensitizers is a promising approach to diverse structural modifications to achieve good light-harvesting properties. Further study on this subject is currently underway in our laboratory.

Acknowlwdgements

This research was partially supported by a Grant-in-Aid for Scientific Research from the Ministry of Education, Science, Sports and Culture of Japan (No. 24655035).

Notes and references

[a] *Department of Applied Chemistry, Graduate School of Urban Environmental Sciences, Tokyo Metropolitan University, 1-1 Minami-ohsawa, Hachioji Tokyo, 192-0397, Japan. Fax &Tel: +81-42-677-3134; E-mail:yujik@tmu.ac.jp*

[b] *Nippon Kayaku Co., Ltd., 31-12, Shimo 3-Chome, Kita-ku Tokyo, 115-8588, Japan.*

† Electronic Supplementary Information (ESI) available: synthesis of intermediates, variable temperature ^1H NMR measurements, electrochemical properties, ATR-FT-IR spectra, and characterization data of dyes. See DOI: 10.1039/b000000x/

1 (a) B. O'Regan and M. Grätzel, *Nature,*1991, **353**, 737; (b) M. Grätzel, *Acc. Chem. Res.*, 2009, **42**, 1788; (c) Y. Ooyama and Y. Harima, *Eur. J. Org. Chem.*, 2009, 2903; (d) A. Hagfeldt, G. Boschloo, L. Sun, L. Kloo and H. Pettersson, *Chem. Rev.*, 2010, **110**, 6595; (e) S. K. Balasingam, M. Lee, M. G. Kang and Y. Jun, *Chem. Commun*., 2013, **49**, 1471.

2 B.-G. Kim, K. Chung and J. Kim, *Chem. Eur. J*., 2013, **19**, 5220.

3 (a) A. Loudet and K. Burgess, *Chem. Rev*., 2007, **107**, 4891; (b) G. Ulrich, R. Ziessel and A. Harriman, *Angew. Chem,. Int. Ed*., 2008, **47**, 1184.

4 N. Boens, V. Leen and W. Dehaen, *Chem. Soc. Rev*., 2012, **41**, 1130.

5 (a) C. Peters, A. Billich, M. Ghobrial, K. Högenauer, T. Ullrich and P. Nussbaumer, *J. Org. Chem*., 2007, **72**, 1842; (b) Z. Li and R. Bittman, *J. Org. Chem.,* 2007, **72**, 8376.

6 L. Bonardi, H. Kanaan, F. Camerel, P. Jolinat, P. Retailleau and R. Ziessel, *Adv. Funct. Mater*., 2008, **18**, 401.

7 (a) S. Erbas, A. Gorgulu, M. Kocakusakogullari and E. U. Akkaya, *Chem. Commun*., 2009, 4956; (b) Y. Cakmak, S. Kolemen, S. Duman, Y. Dede, Y. Dolen, B. Kilic, Z. Kostereli, L. T. Yildirim, A. L. Dogan, D. Guc and E. U. Akkaya, *Angew. Chem., Int. Ed.*, 2011, **50**, 11937; (c) S. G. Awuah and Y. You, *RSC Adv*., 2012, **2**, 11169; (d) A. Kamkaew, S. H. Lim, H. B. Lee, L. V. Kiew, L. Y. Chung and K. Burgess, *Chem. Soc. Rev*., 2013, **42**, 77.

8 (a) O. A. Bozdemir, S. Erbas-Cakmak, O. O. Ekiz, A. Dana and E. U. Akkaya, *Angew. Chem., Int. Ed*., 2011, **50**, 10907; (b) R. Ziessel, G. Ulrich, A. Haefele and A. Harriman, *J. Am. Chem. Soc.,* 2013, **135**, 11330.

9 (a) M. Benstead, G. H. Mehl and R. W. Boyle, *Tetrahedron,* 2011, **67**, 3573; (b) H.-Y. Lin, W.-C. Huang, Y.-C. Chen, H.-H. Chou, C.-Y. Hsu, J. T. Lin and H.-W. Lin, *Chem. Commun*., 2012, **48**, 8913; (c) T. Bura, N. Leclerc, S. Fall, P.Lévêque, T. Heiser, P. Retailleau, S. Rihn, A. Mirloup and R. Ziessel, *J. Am. Chem. Soc*., 2012, **134**, 17404; (d) T. K. Khan, M. Bröring, S. Mathur and M. Ravikanth, *Coord. Chem. Rev*., 2013, **257**, 2348.

10(a) S. Hattori, K. Ohkubo, Y. Urano, H. Sunahara, T. Nagano, Y. Wada, N. V. Tkachenko, H. Lemmetyinen and S. Fukuzumi, *J. Phys. Chem. B,* 2005, **109**, 15368; (b) S. Erten-Ela, M. D. Yilmaz, B. Icli, Y. Dede, S. Icli and E. U. Akkaya, *Org. Lett*., 2008, **10**, 3299; (c) D. Kumaresan, R. P. Thummel, T. Bura, G. Ulrich and R. Ziessel, *Chem. -Eur. J*. 2009, **15**, 6335; (d) C. Y. Lee and J. T. Hupp, *Langmuir,* 2010, **26**, 3760; (e) S. Kolemen, Y. Cakmak, S. Erten-Ela, Y. Altay, J. Brendel, M. Thelakkat and E. U. Akkaya, *Org. Lett*., 2010, **12**, 3812; (f) S. Kolemen, O. A. Bozdemir, Y. Cakmak, G. Barin, S. Erten-Ela, M. Marszalek, J.-H. Yum, S. M. Zakeeruddin, M. K. Nazeeruddin, M. Grätzel and E. U. Akkaya, *Chem. Sci*., 2011, **2**, 949; (g) M. Mao, J.-B. Wang, Z.-F. Xiao, S.-Y. Dai and Q.-H. Song, *Dyes Pigm*., 2012, **94**, 224; (h) K. Gräf, T. Körzdörfer, S. Kümmel and M. Thelakkat, *New J. Chem*., 2013, **37**, 1417; (i) Y. Ooyama, Y. Hagiwara, T. Mizumo, Y. Harima and J. Ohshita, *New J. Chem*., 2013, **37**, 2479; (j) Y. Ooyama, Y. Hagiwara, T. Mizumo, Y. Harima and J. Ohshita, *RSC Adv.,* 2013, **3**, 18099.

11Y. Kubo, Y. Minowa, T. Shoda and K. Takeshita, *Tetrahedron Lett*., 2010, **51**, 1600.

12Y. Kubo, K. Watanabe, R. Nishiyabu, R. Hata, A. Murakami, T. Shoda and H. Ota, *Org. Lett*., 2011, **13**, 4574.

13Y. Zhao, K. Jiang, W. Xu and D. Zhu, *Tetrahedron,* 2012, **68**, 9113.

14N. Sakamoto, C. Ikeda, M. Yamamura and T. Nabeshima, *Chem. Commun*., 2012, **48**, 4818.

15Y. Kubo, K. Yoshida, M. Adachi, S. Nakamura and S. Maeda, *J. Am. Chem. Soc*., 1991, **113**, 2868.

16J. Pommerehne, H. Vestweber, W. Guss, R. F. Mahrt, H. Bässler, M. Porsch and J. Daub, *Adv. Mater*., 1995, **7**, 551.

17A. Hagfeldt and M. Grätzel, *Chem. Rev*., 1995, **95**, 49.

18(a) K. Sayama, K. Hara, N. Mori, M. Satsuki, S. Suga, S. Tsukagoshi, Y. Abe, H. Sugihara and H. Arakawa, *Chem. Commun*., 2000, 1173; (b) T. Horiuchi, H. Miura, K. Sumioka and S. Uchida, *J. Am. Chem. Soc*., 2004, **126**, 12218; (c) C. Teng, X. Yang, C. Yang, S. Li, M. Cheng, A. Hagfeldt and L. Sun, *J. Phys. Chem. C*, 2010, **114**, 9101; (d) W. Lee, J. Y. Seng and J.-I. Hong, *Tetrahedron*, 2013, **69**, 9175.

19A continuous thermal and light soaking stress test using **1**-based cell was carried out under the irradiation of AM1.5G full sun light soaking at 40 °C, where η values were repeatedly measured at several times until about 500 h. As a result, the η value remained at 78% of the initial value for 504 h, meaning that cell has a relatively proper reproducibility and stability for long term.

20Z. Ning and H. Tian, *Chem. Commun.,*2009, 5483.

Novel boron-dibenzopyrromethene dyes with thienyl-cyanoacrylic acid units were synthesized and characterized for application in dye-sensitized solar cells (DSSCs).